A novel transformer-less battery charger for hybrid fuel-cell/photovoltaic electric vehicles based on a new dual-input high step-up DC-DC converter

Pezhman Bayat[1*], Peyman Bayat[2], Abbas Fattahi Meyabadi[3]

[1,2,3] Department of Electrical Engineering, Hamedan University of Technology, Hamedan, Iran

ARTICLE INFO	ABSTRACT
	The hydrogen fuel cell is one of the latest technologies used in fuel cell electric vehicles (FCEVs), which uses hydrogen gas to supply the electrical energy needed by the electric engines. One of the important challenges of FCEVs is that if the battery is fully discharged, there must be a structure that can charge the battery with high efficiency through fuel cells or other sources. Otherwise, charging stations should be placed for such vehicles in many parts of the country, and on the other hand, high-capacity batteries should be installed for them. Based on this, in this article, a novel dual-input single-output high step-up converter with high efficiency is presented, which is able to simultaneously charge the battery with fuel cells and solar energy. The proposed topology has boost function and uses a novel diodes and switches network, which leads to the creation of an integrated system with high efficiency and high voltage gain. Other advantages of the proposed converter are small size, low voltage and current stresses on all the components, less component count, continuous input current and light weight; which makes it more efficient compared to existing structures. In this regard, theoretical calculations and steady state analysis for the proposed system have been presented. Also, in order to verify the performance of the proposed converter, it has been simulated in the MATLAB/Simulink software environment at the rated power of 1kW, with an output voltage of 220V and an output current of 4.55A, and the results have been presented in detail. The peak efficiency of the proposed converter reached 97.4% at half power, and the efficiency at rated power was reported 96%. Moreover, in the proposed structure, the voltage stress of capacitors, diodes and switches reaches the maximum value of 63%, 83% and 41% of the output voltage, respectively; which are promising values. Finally, to verify the performance of the proposed converter and the relationships obtained, a 1kW prototype is built in the laboratory to demonstrate the efficiency of the proposed converter.

1. Introduction

Fossil fuels are a non-renewable source of energy and they bring environmental problems such as air pollution and have low energy production efficiency. Because renewable energy resources are easy to access and free to use, and also have relatively higher efficiency than fossil resources, so, today the energy sources used are changing from fossil sources to renewable sources such as photovoltaics (PVs), wind energy and etc. But each of these sources has limitations due to its own structure. For example, PV does not produce energy at night; Therefore, in order to provide stable and permanent energy and increase the reliability, these sources can be connected together and with special structures, their energy production can be delivered to the load. In addition, the

* Corresponding Author: Pezhman Bayat
Email Address: pezhman.bayat@hut.ac.ir
https://doi.org/10.22068/ase.2024.656

connection of multiple sources in the system provides the basis for studying optimal issues [1]. The problem of coordinating and providing a mechanism for energy transfer from energy production sources to the consumer or consumers, as well as energy exchange between energy storage sources (batteries) and the system can be solved by using multi-input multi-output (MIMO) DC/DC converters [2]. In line with these goals, various topologies and structures have been presented in this field, each of which has its own limitations and advantages. Fuel cell electric vehicles (FCEVs) as a newly emerging technology can provide the power required for traction motor by using renewable resources in addition to the fuel cells (FCs) [3]. Therefore, it is very important to use the high efficiency converter for energy management in these types of vehicles.

2. Related Works and Literature Review

In this section, the existing literature and related works in the field of MIMO converters are reviewed and presented, and the advantages and disadvantages of each are stated. In general, the topologies of MIMO converters used in FCEVs can be categorized into three topologies: the first category is converters with magnetic coupling, the second category is converters with electrical coupling, and the third category is hybrid converters [4, 5]. In the converters of the first category, there is a multi-coil transformer that receives the primary coils of electrical energy and converts it into a magnetic field in the core. This field creates a voltage in the secondary and tertiary windings and is given to the load, and thus electrical energy is received from the input sources and transferred to the output. In electric type converters, there is no isolation between input and output. These converters are offered in non-isolated converters such as buck and boost. The control of these converters is done with the working period of the switches, and they have high power of energy transmission. The third category is a combination of the previous two categories that have the advantage of isolation and easy control at the same time [4];

The isolated buck-boost dual-input single-output (DISO) converter is the first and simplest topology for this category of converters [6]. In this topology, the transformer has two roles, the first one can act as a buck or boost agent, and the second one is to gather energy from input sources in the form of field flow. In this topology, two sources cannot inject power to the load at the same time, and this is considered one of the disadvantages of this converter, however, this converter has a very simple structure and its control is easily possible,

but the inability to charge the battery and the lack of attention to soft switching is one of the disadvantages of the converter. Two-input full-bridge converters are another widely used converters in electric vehicles that work on the basis of magnetic field [7]. In this type of converters, the primary side mainly uses current source converters, and the output rectifier is usually a full bridge structure. The disadvantage of this type of converters is high losses, the number of components and its big dimension due to the use of transformers.

In [8], a novel DISO converter family is presented, obtained by embedding a general cell into buck–boost and classic buck converters. The main disadvantages of this converter are a limited voltage gain and low efficiency. In [9], a novel DISO converter was presented based on two traditional boost converters combining with two active clamp circuits and coupled inductors, which provided two separate power flow paths from each input port to the output load. Indeed, two boost converter were placed in parallel and some components played common roles to reduce the number of converter elements. This issue leads to the fact that the overall power is strongly dependent on the power status of each of the inputs, so that if one source has a problem, then the overall system status becomes unstable.

Series and parallel structures are also widely used in multi-input converters. In the article [10], a structure is presented that is designed to combine two sources of electrical energy and is presented in two types of series and parallel, which in the series type, the flow current of the two converters is equal. But because the voltages are in series, it is difficult to control the output voltage. In addition, the occurrence of problems in any of the converters can cause a total interruption of energy transfer to the load. Another converter is presented in the article [11], where two input sources are connected to the battery using a boost converter and to the output using a full bridge converter, respectively. This converter has a simple structure, but its voltage gain is limited.

In [12], the structure of the two-input converter with three power switches is presented. In this topology, the battery is regularly charged and discharged, which is one of the disadvantages of this converter; On the other hand, one of its advantages is soft switching, thus causing the switching loss in this converter to be low and the converter can be used for cases with high power switching. In [13], a non-isolated MIMO converter is designed for electric vehicles, where an energy storage source such as a battery and FCs are placed

together; However, the voltage level of the battery must always be higher than the FCs, which is considered a big disadvantage. A novel DISO DC-DC converter based on quasi-Z source is presented in [14]. This topology is a suitable converter for efficiently interfacing two input sources with a common load. The proposed converter, by integrating the coupled-inductor and switched-capacitor cell provides a high voltage gain at small duty cycles. The main disadvantage of this structure is the existence of a coupled inductor, which increases the overall dimensions and weight. As a summary, the positive and negative features of the investigated converters are listed in Table 1.

2.1. Research Gap

According to the studies conducted in Section 2 and the review of the existing literature, it can be stated that the structures that have been presented so far have deficiencies that can be mentioned as follows: 1) Limited performance; 2) Limited voltage gain; 3) High number of components; 4) Complicated design; 5) High voltage stress of switches; 6) High voltage stress of diodes; 7) High number of components and 8) High input current ripple. These defects are separately listed in Table 1 for each converter. In addition to the disadvantages mentioned in the studied structures, in order to have a high voltage gain, it is necessary to have a high duty cycle of the power switches; which increases losses and reduces the lifespan of switches. In addition, high voltage and current stresses increase losses and costs. Accordingly, there is a research gap in the existing literature to provide a structure that can achieve high voltage gain at low duty cycle and simultaneously have two inputs. In addition to the mentioned advantages, in the proposed converter, the number of components should be less, the efficiency should be higher, and the voltage and current stresses of the components should be lower.

2.2. Contribution and Organization

This paper proposes a novel DISO high step-up DC-DC converter that considers the different requirements of new energy generation systems for dual-input converters for FC/PV electric vehicle without using any coupled inductor and transformers.

Table 1: Comparison of existing topologies of the MIMO DC–DC converters

Refs.	Max. Duty Cycle of the Switches	Number of Components	Pros (+ → ■) and Cons (− → ❖)
[6]	100%	11	❖ Limited performance ❖ Limited voltage gain ■ Triple input possibility ■ Magnetically isolated
[7]	100%	22	❖ High number of components ❖ Complicated design ■ Three-winding transformer ■ Magnetically isolated
[8]	100%	11	❖ High voltage stress of switches ❖ Limited voltage gain ❖ Limited performance ■ Simple structure
[9]	100%	17	❖ High number of components ❖ High voltage stress of diodes ■ Continuous input current
[10]	100%	12	❖ Limited voltage gain ❖ High voltage stress of diodes ■ Continuous input current ■ Double input possibility
[11]	100%	9	❖ High input current ripple ❖ Limited voltage gain ■ Triple input possibility ■ Simple structure
[12]	100%	9	❖ Limited voltage gain ■ Continuous input current ■ Triple input possibility
[13]	100%	11	❖ High number of components ❖ Limited voltage gain ■ Simple structure
[14]	50%	14	❖ High number of components ■ High voltage gain ■ Magnetically isolated ■ Continuous input current ■ Double input possibility

A novel transformer-less battery charger based on a new dual-input high step-up DC-DC converter

Figure 1: Hybrid FC/PV electric vehicle power flow based on a proposed dual-input high step-up DC-DC converter.

The proposed topology has two input sources, boost function, and a novel diodes and switches network, which leads to the creation of an integrated system with high efficiency and high voltage gain. Moreover, the proposed network structure reduces the voltage stress on the capacitors and all diodes. Other advantages of the proposed topology are small size, low voltage and current stresses on all the components, less component count, continuous input current and light weight. According to Fig. 1 and as mentioned earlier, this converter is generalized for FC/PV electric vehicle applications. However, it can be used in all hybrid energy applications.

In summary, the innovations of the present article are as follows:

- A novel DISO high step-up DC-DC converter is provided with unique features for FC/PV electric vehicle applications;

- The proposed topology has a novel diodes and switches network, which leads to the creation of an integrated system with high efficiency and high voltage gain;

- The proposed network structure reduces the voltage stress on the capacitors and all diodes;

- The proposed topology has unique features such as small size, low voltage and current stresses on all the components, less component count, continuous input current and light weight;

- In the proposed converter, the inputs are able to supply the load together or individually, which increases the reliability of the converter;

- In addition to the fact that the converter has been developed for FCEVs, however, the high voltage gain and low losses in the converter have made it possible to use it in industry and renewable energy;

- In order to confirm the proposed structure, in addition to complete theoretical calculations, the converter for the input of 24V PV panel and 48V FC module has been simulated in the MATLAB/Simulink software environment and the results have been presented and compared with the theoretical results.

The rest of this paper is organized as follows. In the Section 3, the structure of the proposed DISO converter is given in detail. Operating modes of the proposed DISO converter and derivation of voltage gain are presented in Section 4. Section 5 provides derivation of voltage stresses on the components. Efficiency analysis is reported in Section 6. The simulation and experimental results of the proposed converter and comparative analysis are completely shown in Sections 7 and 8. Finally, Section 9 concludes this paper.

3. Proposed DISO High Step-up DC-DC Converter

In this section of the paper, the structure and components of the proposed DISO high step-up converter are given in detail. The proposed topology is shown in Fig. 2, which is composed of L_{in} as an input inductor, S_1, S_2 and S_3 as three metal-oxide-semiconductor field-effect transistors (MOSFETs); Furthermore, there are three capacitors (C_1, C_2 and C_3) and five diodes (D_1, D_2, D_3, D_{in} and D_O) in the proposed topology.

Capacitors C_2 and C_3 assume the task of supplying the load in different duty cycles and supply the load.

In the design of the proposed converter, D_O, C_2 and C_3 are considered as output filters, so that when the MOSFETs are turned OFF and ON, capacitor C_2 and C_3 are charged and discharged and supply the load. V_{FC} and V_{PV} are used as the input voltages to display the FC and PV voltages. The suggested work mode of the converter is continuous current mode (CCM). Fig. 2 shows the circuit configuration of the proposed high step-up converter. Also, Fig. 3 shows the operating modes of the proposed topology. The typical voltage/current waveforms in the CCM mode for this DISO high step-up converter are shown in Fig. 4.

4. Operating Modes of the Proposed DISO Converter

The detailed analysis of the proposed converter is on the assumptions of [3]:

- All the calculations are in the CCM.

- The power MOSFETs and the diodes are ideal switches.

- Input inductor and all of the capacitors are linear, time invariant, and frequency independent.

- The capacitors voltages are constant in a switching period.

Figure 2: Proposed transformer-less dual-input high step-up DC-DC converter.

There are two operating modes of the proposed converter in one switching period, as shown in Fig. 4.

Mode I [t₀, t₁]: In this mode, as shown in Fig. 3(a), the switches S_1, S_2 and S_3 are in ON state; the input inductor (L_{in}) stores energy from input source V_{FC} and the voltage across L_{in} is $V_{FC} + V_{C1}$. The input inductor current i_{Lin} increases linearly. The diodes D_{in}, D_1, D_2 and D_3 are in OFF state, while the diode D_o is in ON state. By applying Kirchhoff's voltage law (KVL) on the circuit in Fig. 3(a), following equations are obtained.

$$V_{Lin}^{Mode\,I} = V_{FC} + V_{C1} = V_{C3} \qquad (1)$$

$$V_O^{Mode\,I} = V_{C2} + V_{C3} \qquad (2)$$

Mode II [t₁, t₂]: In this mode, as shown in Fig. 3(b), the switches S_1 and S_2 are in ON state; while the switch S_3 is in OFF state. L_{in} stores energy from input source V_{PV} and the voltage across L_{in} is $V_{PV} + V_{C1}$. Since the voltage level of the PV panel is lower than that of the FC module, So, the current of the input inductor current (i_{Lin}) increases with a lower slope than in the first mode of operation. Furthermore, similar to the first mode, the diodes D_1, D_2 and D_3 are in OFF state, while the diodes D_o and D_{in} are in ON state. By applying KVL on the circuit in Fig. 3(b), following equations are obtained.

$$V_{Lin}^{Mode\,II} = V_{PV} + V_{C1} = V_{C3} \qquad (3)$$

$$V_O^{Mode\,II} = V_{C2} + V_{C3} \qquad (4)$$

Mode III [t₂, t₃]: At t₂, switches S_1 and S_2 receive the turn OFF signal and start to turn OFF. The switch S_3 is still OFF. So, all switches are OFF. D_{in}, D_1, D_2 and D_3 are in ON state, while the diode D_o is in OFF state. The voltage across L_{in} is $V_{PV} - V_{C1}$ and the input inductor current (i_{Lin}) decreases. By applying KVL on the circuit in Fig. 3(c), following equations are obtained.

$$V_{Lin}^{Mode\,III} = V_{PV} - V_{C1} \qquad (5)$$

$$V_{C1} = V_{C2} \qquad (6)$$

$$V_O^{Mode\,III} = V_{C2} + V_{C3} \qquad (7)$$

3.1. Derivation of Voltage Gain

The symbols D_m, *and* D_3 are defined as the switches $S_{1,2}$, and S_3 duty cycles, respectively. In the proposed converter both inputs V_{FC} and V_{PV} are involved in transferring energy to the battery. The volt–second balance principle applies to the input inductor L_{in}. Therefore, the L_{in} average voltage in one period of switching can be expressed as
$V_{Lin}^{Mode\,I} d^{Mode\,I} + V_{L_1}^{Mode\,II} d^{Mode\,II} +$

$V_{L_1}^{Mode\ III} d^{Mode\ III}$; so, considering that the average voltage of the input inductor in a switching period is equal to zero, we have:

$$\langle V_{Lin} \rangle_T = 0 \rightarrow \left(V_{Lin}^{Mode\ I} \right) D_3$$
$$+ \left(V_{Lin}^{Mode\ II} \right) (D_m - D_3)$$
$$+ \left(V_{Lin}^{Mode\ III} \right) (1 - D_m) \qquad (8)$$
$$= 0$$

So, using (1), (3) and (5), $\langle V_{Lin} \rangle_T$ can be calculated as follows:

$$\langle V_{Lin} \rangle_T = (V_{FC} + V_{C1}) D_3$$
$$+ (V_{PV} + V_{C1})(D_m - D_3)$$
$$+ (V_{PV} - V_{C1})(1 - D_m) \qquad (9)$$
$$= 0$$

By simplifying (9), we have:

$$V_{C1} = V_{C2} = \frac{V_{FC} D_3 + V_{PV}(1 - D_3)}{1 - 2D_m} \qquad (10)$$

Also, the average amount of output voltage in one switching period is as follows:

$$\langle V_O \rangle_T = V_{C2} + V_{C3} \qquad (11)$$

By combing the equations (1) and (11), the output voltage can be expressed as follows.

$$V_O = V_{C2} + V_{FC} + V_{C1} \qquad (12)$$

Using (10) and (12), the voltage gain can be determined by the following equation.

$$V_O = \left(\frac{0.5 + D_3 - D_m}{0.5 - D_m} \right) V_{FC}$$
$$+ \left(\frac{1 - D_3}{0.5 - D_m} \right) V_{PV} \qquad (13)$$

5. Derivation of Voltage Stresses on the Components

By using (3) and (10), the voltage stress across the capacitors C_1, C_2 and C_3 can be obtained as:

$$V_{C1}^{Peak} = V_{C2}^{Peak} =$$
$$= \left(\frac{D_3}{1 - 2D_m} \right) V_{FC} \qquad (14)$$
$$+ \left(\frac{1 - D_3}{1 - 2D_m} \right) V_{PV}$$

$$V_{C3}^{Peak} = V_{FC} + V_{C1}^{Peak}$$
$$= \left(\frac{1 + D_3 - 2D_m}{1 - 2D_m} \right) V_{FC} \qquad (15)$$
$$+ \left(\frac{1 - D_3}{1 - 2D_m} \right) V_{PV}$$

Also, the voltage stresses of all of the switches and diodes for presented topology are given as follows:

$$V_{S1}^{Peak} = V_{S2}^{Peak} = V_{PV} - V_{Lin}^{Mode\ III}$$
$$= V_{PV} + V_{C1} - V_{PV} = V_{C1}$$
$$= \left(\frac{D_3}{1 - 2D_m} \right) V_{FC} \qquad (16)$$
$$+ \left(\frac{1 - D_3}{1 - 2D_m} \right) V_{PV}$$

$$From\ Modes\ II\ and\ III: V_{S3}^{Peak}$$
$$= V_{FC} - V_{PV} \qquad (17)$$

$$From\ Mode\ I: V_{Din}^{Peak} = V_{FC} - V_{PV} \qquad (18)$$

$$From\ Modes\ II\ \&\ III: V_{D1}^{Peak} = V_{D2}^{Peak}$$
$$= V_{C1}^{Peak} =$$
$$= \left(\frac{D_3}{1 - 2D_m} \right) V_{FC} \qquad (19)$$
$$+ \left(\frac{1 - D_3}{1 - 2D_m} \right) V_{PV}$$

$$From\ Modes\ II\ \&\ III: V_{D3}^{Peak} = V_{C2}^{Peak}$$
$$= \left(\frac{D_3}{1 - 2D_m} \right) V_{FC} \qquad (20)$$
$$+ \left(\frac{1 - D_3}{1 - 2D_m} \right) V_{PV}$$

$$From\ Mode\ III: V_{Do}^{Peak}$$
$$= -V_{Lin}^{Mode\ III} + V_{C3}^{Peak}$$
$$= V_{C1}^{Peak} + V_{C3}^{Peak} - V_{PV}$$
$$= \left(\frac{2D_3}{1 - 2D_m} \right) V_{FC} \qquad (21)$$
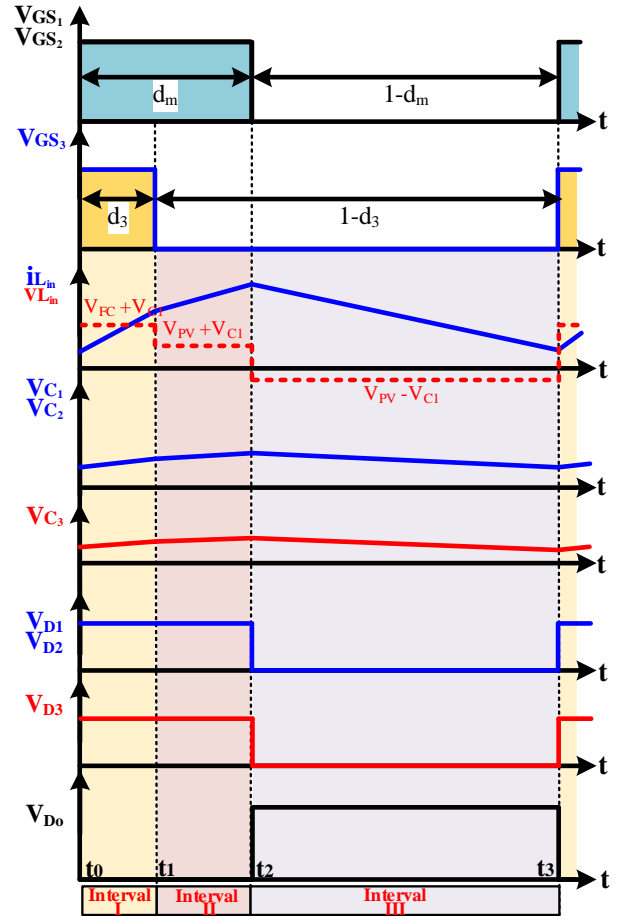$$+ 2 \left(\frac{1 - D_3}{1 - 2D_m} \right) V_{PV}$$

Figure 4: Typical waveforms of the components.

6. Efficiency Analysis

The power loss of the proposed topology is composed of the power dissipation of switches, diodes, magnetizing element, and capacitors.

Power dissipations of the switches are composed of conduction loss and switching loss, which can be expressed as [3, 14]:

$$P_S = \sum_{i=1}^{3} P_{cond,Si} + P_{SW,Si}$$
$$= \sum_{i=1}^{3} r_{Si} I_{Si-RMS}^2 \qquad (22)$$
$$+ \frac{1}{6} V_{Si} f_{si} I_{si}(t_{on} + t_{off})$$

where r_{si} is the MOSFETs ON-resistance; $P_{cond,Si}$ is conductive losses; $P_{SW,Si}$ is switching losses; I_{Si-RMS} is root mean square of MOSFETs; f_{si} is switching frequency; t_{on} is MOSFET turn-on time and t_{off} is MOSFET turn-off delay time.

Also, the diodes power losses are:

$$P_D = \sum_{i}^{1,2,3,in,o} r_{Di} I_{Di-RMS}^2 + V_{FDi} I_{Di-avg} \qquad (23)$$

Figure 3: Operating modes of the proposed converter; (a) Mode 1, (b) Mode 2, and (c) Mode 3.

Automotive Science and Engineering (ASE)   4274

where r_{Di} is the diode forward resistance; V_{FDi} is the diodes threshold voltages and I_{Di-avg} is average diode current.

The losses in input inductor L_{in} and capacitors are:

$$P_{Lin} = r_{Lin}I_{Lin-RMS}^2 \qquad (24)$$

$$P_C = \sum_{i=1}^{3} r_{Ci}I_{Ci-RMS}^2 \qquad (25)$$

where r_{Lin} is the equivalent series resistance (ESR) of the input inductor L_{in} ; r_{Ci} is the ESR of the capacitors; $I_{Lin-RMS}$ is RMS current of input inductor and I_{Ci-RMS} is RMS current of capacitors.

Hence, the overall power loss of the proposed converter is:

$$P_{Loss}^{Total} = P_S + P_D + P_{Lin} + P_C \qquad (26)$$

Finally, the calculated efficiency of the proposed converter can be calculated by:

$$\eta = \frac{P_o}{P_{in}} = \frac{P_o}{P_o + P_S + P_D + P_{Lin} + P_C} \qquad (27)$$

7. Simulation and Experimental Results

In this section, simulation and experimental results are presented to verify the performance of the proposed DISO converter. The simulation was done in the Simulink environment of MATLAB software and the parameters used in the simulation and experimental prototype are presented in Table 2.

7.1. Simulation Results

To achieve simulation results, the input voltage of the PV panel (V_{PV}) was considered equal to 12 volts and the input voltage of the FC module (V_{FC}) was considered equal to 24 volts. Also, the switching frequency is equal to 70 kHz. In the simulation results, the key waveforms of the proposed converter, including PWM signals for switches S_1, S_2 and S_3, the voltage and current of the input inductor (V_{Lin} and I_{Lin}), the output voltage and current (V_o and I_o) and the voltages of the diodes (V_{D1}, V_{D2}, V_{D3} and V_{Do}) were extracted and shown in Figs. 5(a)-(e). The duty cycle of the MOSFET S_3 is equal to 15% and the MOSFETS S_1 and S_2 are simultaneously set to 35%; and the results are extracted with fixed duty cycles (see Fig. 5(a)).

Table 2: Parameters of the proposed converter used to derive simulation and experimental results

Parameters	Values
PEMFC voltage (V_{FC})	$48V$
PV Voltage (V_{PV})	$24V$
Output voltage	$220V$
Max. output power (P_{out}^{max})	$1KW$
$S_{1\sim3}$	MOSFET; IRFP4668PbF with $R_{DS}(ON) = 8m\Omega$; $T_{d,on} = 41ns, T_{d,off} = 64ns$; $V_{DSS} = 200V$; $I_D = 130A$
$D_{1\sim3}, D_{in}$	Ultrafast diode; RURP3020, $200V/30A$; $r_D = 0.03\Omega$; $V_F^{max} = 1V$
D_O	Ultrafast diode; RURP3060, $600V/30A$; $r_D = 0.04\Omega$; $V_F^{max} = 1.5V$
C_1, C_2 and C_3	$120\mu F/200V$, with $r_c = 82m\Omega$
Switching frequency (f_s)	$70KHz$
L_1	$220\mu H$ with $r_L = 0.2\Omega$

From Fig. 5(b), peak voltage and average current of the input inductor (V_{Lin} and I_{Lin}) are 133.35V and 30A, respectively. Also, as shown in Fig 5(c), the output voltage and load current are equal to 218.5V and 4.36A, respectively. Since the voltage of the FC is assumed equal to 48V and the voltage of the solar cell is assumed equal to 24V, and also the value of the duty cycle for the first and second MOSFETs is equal to 35% and the value of the duty cycle for the third MOSFET is equal to 15%, then based on (13), the output voltage value of 232V is obtained; which is equal to the simulation value with high accuracy. The reason for the difference is that the parasitic resistances of capacitors, input inductors, diodes, and the ON-state resistances of MOSFETs have been neglected in the calculation of the voltage gain according to the assumptions of the present study. According to the simulation results presented in Fig. 5(d), the peak voltages of the diodes indicated by V_{Din}^{Peak}, V_{D1}^{Peak}, V_{D2}^{Peak}, V_{D3}^{Peak} and V_{Do}^{Peak} are 23.3V, 85V, 87.2V, 87V and 174V, respectively. These results are equal to the theoretical calculations presented in (18) to (21).

Also, the voltage stresses on the components are derived and shown in Fig. 6. The peak efficiency reaches 97.4% at half power, and the efficiency at rated power is 96%. According to simulation results, the proposed converter has advantages of high voltage gain, the least number of components, continuous input current, and common ground.
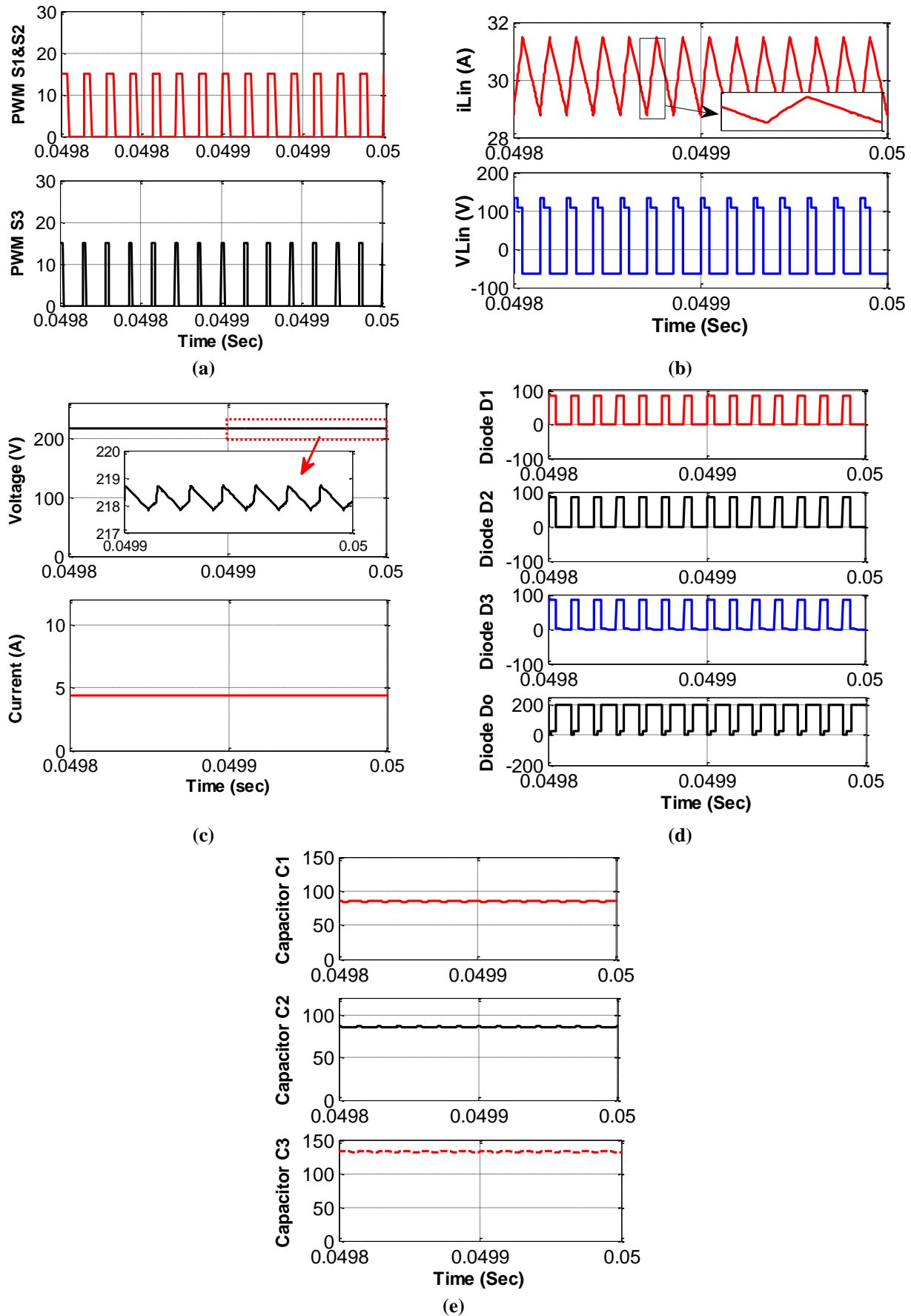
4275   Automotive Science and Engineering (ASE)

(a)

(b)

(c)

(d)

(e)

Figure 5: Simulation Results: (a) PWM signals for switches; (b) Voltage and current of the input inductor (V_{Lin} and I_{Lin}); (c) Output voltage and current (V_o and I_o); (d) Voltages of the diodes (V_{D1}, V_{D2}, V_{D3} and V_{Do}); (e) Voltages of the capacitors (C_1, C_2 and C_3).
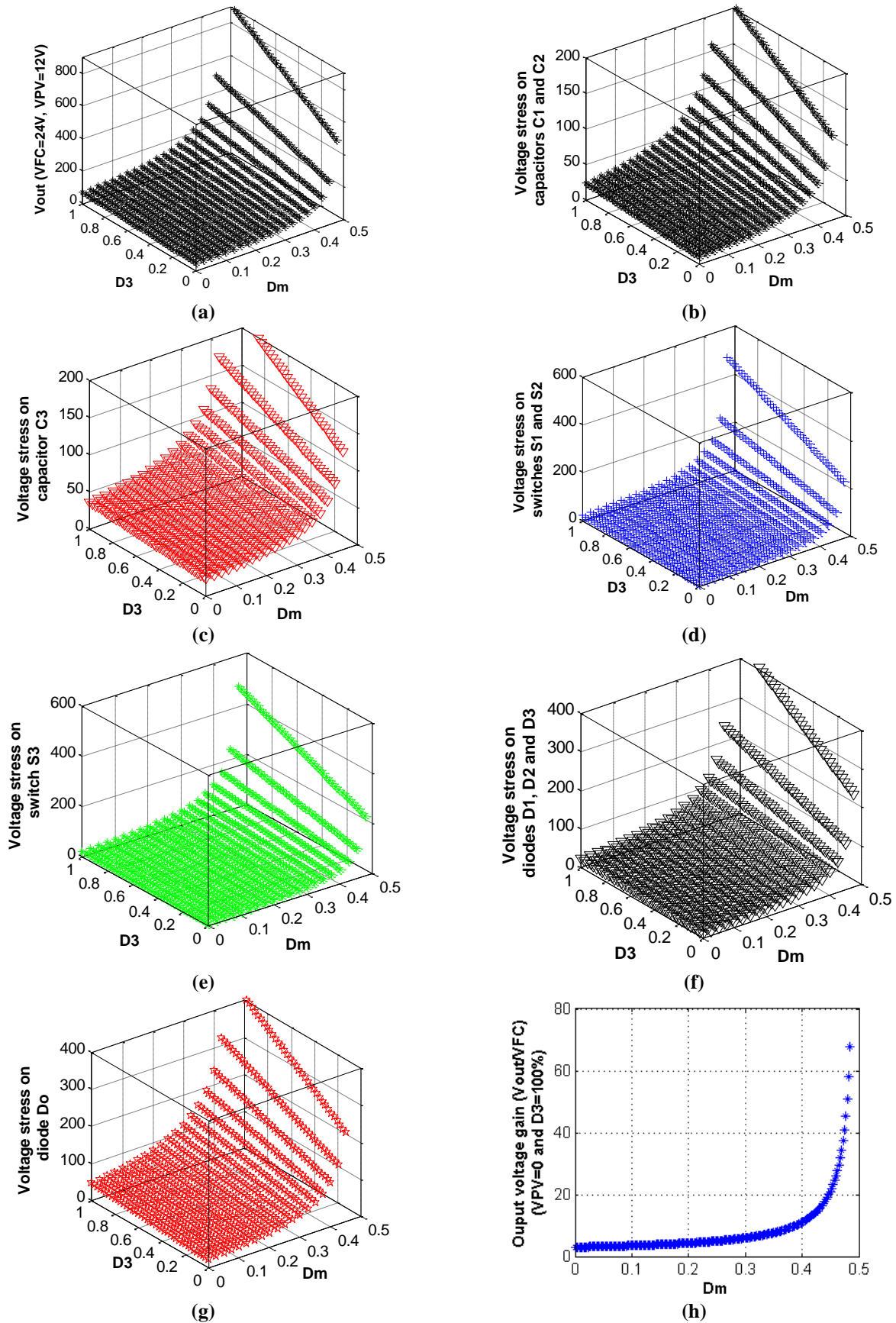
Figure 6: Voltage stresses on the components; (a) V_{out}; (b) C_1 and C_2; (c) C_3; (d) S_1 and S_2; (e) S_3; (f) V_{D1}, V_{D2} and V_{D3}; (g) V_{Do}; and (h) V_{out}/V_{FC}.

``Also, the voltages of the capacitors (C_1, C_2 and C_3) were extracted and shown in Fig. 5(e). According to the simulation results, capacitors with suitable voltage and low cost can be selected, which reduces the total operating cost. According to the simulation results in Fig. 5(e), the peak voltages of the capacitors indicated by V_{C1}^{Peak}, V_{C2}^{Peak} and V_{C3}^{Peak} are 87.5V, 87.5V and 132.8V, respectively. These values are equal to the theoretical calculations presented in (14) and (15).

So, based on simulation results, the proposed topology is useful in FCEVs applications because of its simple structure, high voltage gain, low input current ripple, common ground, and high efficiency. It is noteworthy that, the simulation results agree well with the theoretical analysis of the converter.

In order to show the accuracy of theoretical calculations, simulation results and theoretical results are listed side by side in Table 3. According to the results, it is clear that the results of simulation and theoretical calculations are close to each other with high accuracy.

Table 3: Comparison of simulation results and theoretical calculations

Parameters	Theoretical Calculations	Simulation Results
V_{C1}^{Peak}	From (14): 92V	87.5V
V_{C2}^{Peak}	From (14): 92V	87.5V
V_{C3}^{Peak}	From (15): 140V	132.8V
V_{S1}^{Peak}	From (16): 92V	87.5V
V_{S2}^{Peak}	From (16): 92V	87.2V
V_{S3}^{Peak}	From (17): 24V	23.3V
V_{Din}^{Peak}	From (18):24V	23.3V
V_{D1}^{Peak}	From (19): 92V	85V
V_{D2}^{Peak}	From (19): 92V	87.2V
V_{D3}^{Peak}	From (20): 92V	87V
V_{Do}^{Peak}	From (21): 184V	174V
V_O	From (13): 232V	218.5V

7.2. Experimental Results

In this section, in order to confirm the theoretical calculations and simulation results that were presented in the previous sections, the proposed system has been built and the results obtained from the construction of a 1kW prototype in the laboratory are provided. Fig. 7 shows the experimental setup of the proposed converter prototype.

Fig. 8 shows experimental waveforms of voltages/currents for $V_{GS-S_{1,2,3}}$, i_{L_1}, V_{out}, i_{out} and $V_{C1,C2,C3}$. According to Fig. 8(b), it is clear that the input inductor current (i_{L_1}) increases with an

upward slope when the MOSFETs are ON, and decreases on the opposite side when the MOSFETs are turned OFF. It is also clear that the peak-to-peak current ripples in the input inductor are very low and it is about 2.5A even if the system is working at high power and since these stresses transfer on the input sources; therefore, the stresses on the input sources are low and their lifespan increases significantly.

In Figs. 8(c) and (d), the experimental voltage stresses on the capacitors V_{C1}, V_{C2} and V_{C3} at $P_o = 1000W$ are extracted and depicted. These waveforms show that the voltage stresses of the capacitors are $88V$, $88V$ and $133V$, respectively. Based on the results, it is clear that the obtained values are significantly equal in theoretical calculations, simulation and experimental results. It is again confirmed that the proposed converter is appropriate for the practical applications.
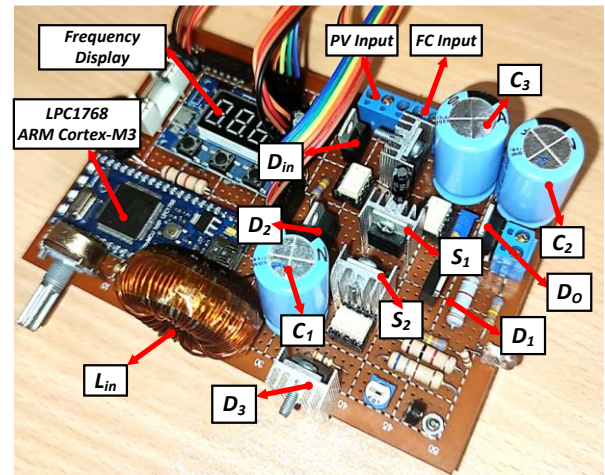

Figure 7: Experimental prototype device of the proposed dual-input high step-up DC-DC converter.

7.3. Efficiency and Power Losses Analysis

The theoretical efficiency curve (based on Section 6), the efficiency curve obtained from the simulation in the MATLAB/Simulink software environment and the efficiency curve obtained from experimental results of the proposed topology as a function of the output power P_O at the input voltages of $V_{FC} = 48V$ and $V_{PV} = 24V$ are shown in Fig. 9. Among the three results, on average, the peak efficiency reached 97.4% at half power, and the efficiency at rated power was reported 96%. Also, a percentage diagram to show component power losses is shown in Fig. 10. Obviously, the highest losses are related to power switches and diodes.
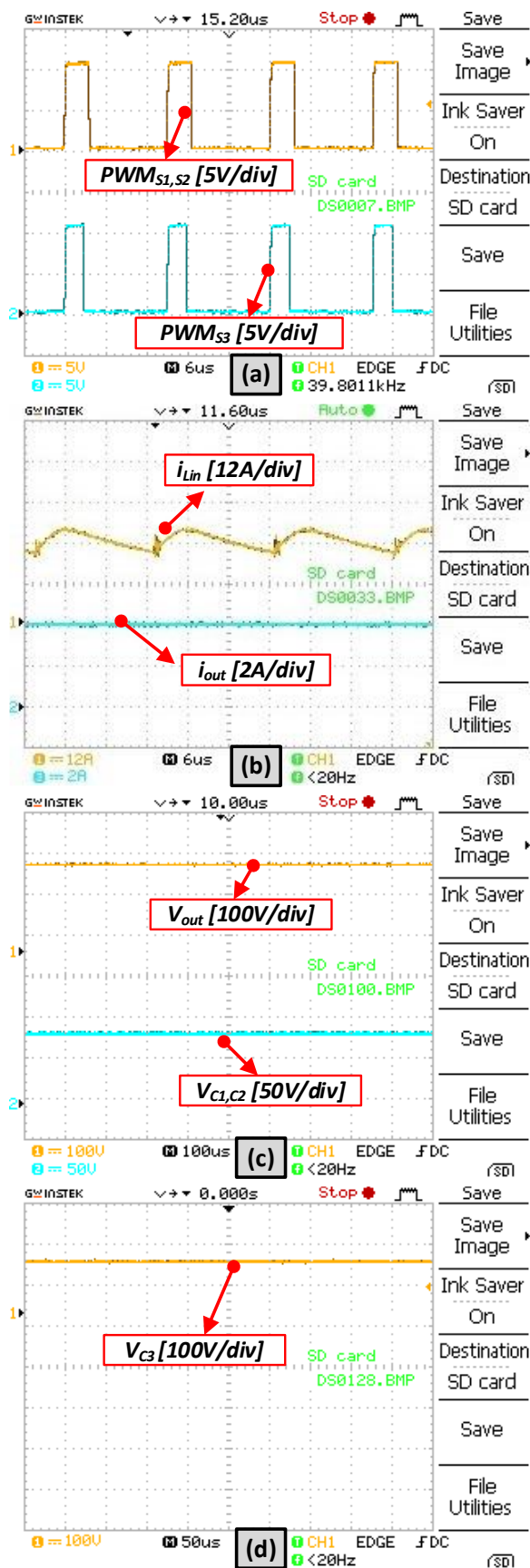
7.4. Design limitations and future studies

FCs can become unstable against oxygen and hydrogen pressure changes. Also, the cold temperature of the environment can disturb the performance of the system. Based on this, providing a suitable controller to absorb maximum power is on the agenda of future works by the researchers of this article. Also, making a laboratory prototype at higher power can be accompanied by challenges in practice; the initial steps have been taken in this field, and the results of the work will be presented in the future papers by the researchers of this article. Moreover, the main purpose of this article is to present the topology itself and focus on a structure that has very low voltage and current stresses on diodes and power switches. This claim has been proven based on theoretical calculations and simulation. Although the protection circuits are issues that cannot be ignored and will be considered in future works on the presented structure. Indeed, snubbers are necessary to prevent damage to semiconductors due to electrical stress from transient oscillations of voltage and current waves. Also, snubbers for diodes help during the reverse recovery process, in which over voltages occur.
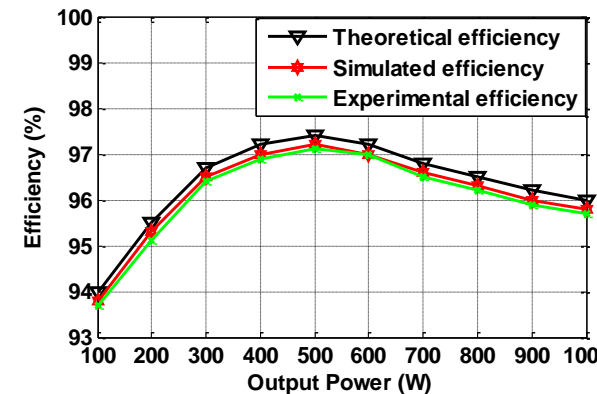

Figure 9: Comparison theoretical efficiency curve and the efficiency curve obtained from the simulation and experimental results.
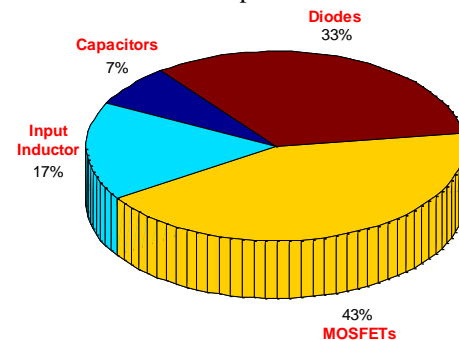

Figure 10: Percentage loss distribution of the proposed converter.

Figure 8: Experimental results: (a) PWMs for S_1, S_2 and S_3; (b) i_{Lin} and i_{out}; (c) V_{out}, V_{C1} and V_{C2}; (d) V_{C3}.

8. Comparative Analysis

In this section, the proposed DISO high step-up DC-DC converter is compared with other related converters which presented in [2], [3] and [14]. All these converters have an impedance network and have a coupled-inductor; furthermore, selected converters can be used in high step-up applications e.g., fuel cell-based battery chargers. Table 4 gives the comparing results from different aspects including structure, number of ports, maximum efficiency and pros and cons. A converter in [2] uses a modified quasi z-source impedance network. This converter has some additional advantages compared to the other related converters, e.g. (1) using the coupled inductor technique, thus providing a high voltage gain; (2) imposing low voltage stress on components; (3) utilizing small duty cycle with extremely high voltage conversion ratio and high efficiency; (4) having continuous input current with small ripples, which makes the converter suitable for FC applications; and (5) increasing reliability and using only one power MOSFET. Despite the mentioned advantages, this converter uses a coupled-inductor that increases the losses and leads to a decrease in efficiency. Also, as mentioned earlier, the use of magnetic devices such as coupled-inductors and transformers lead to increasing the cost and dimensions. Converter in [3] and [14], also use a modified quasi z-source impedance network using the switched capacitors and coupled-inductor techniques, which result in a high voltage gain; these converters have resolved the voltage gain limitation issue in the basic z-source impedance network but have preserved its main advantages; and also, they have three ports for hybridizing PV panels, rechargeable batteries and isolated loads. Despite the mentioned advantages, these converters also use a coupled-inductor that increases the losses and leads to a decrease in efficiency. So, in summary, the converters in [2], [3] and [14], have higher hardware costs and larger volumes due to the use of coupled-inductor. Moreover, their efficiency and stability are limited due to some factors such as weight, losses and coupling coefficients.

In comparison to mentioned converters, the proposed non-isolated high-gain DC-DC converter holds tremendous potential in the field of power conversion technology. Its' strong boosting capability, small volume and weight, high efficiency and good adjustability has made it a good choice in DISO battery chargers; the proposed topology has a novel diodes and switches network, which leads to the creation of an integrated system with high efficiency and high voltage gain; also, the proposed network structure reduces the voltage stress on the capacitors and all diodes; moreover, the proposed topology has unique features such as small size, low voltage and current stresses on all the components, less component count, continuous input current and light weight. Also, not using transformers and coupled-inductors has led to increasing the efficiency and reducing losses in the presented converter, which has achieved an efficiency of 97.4%.
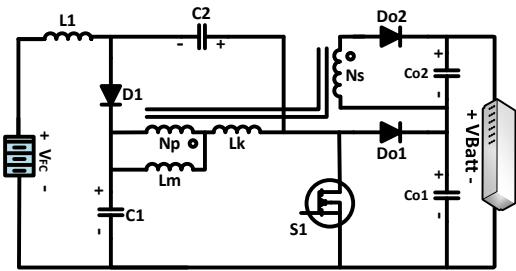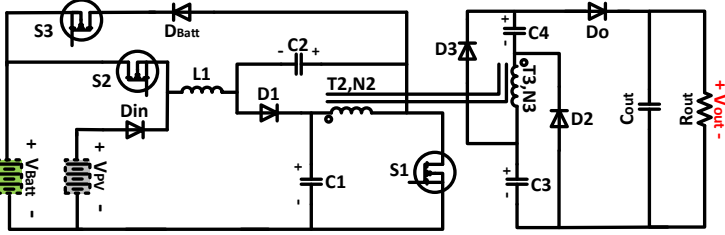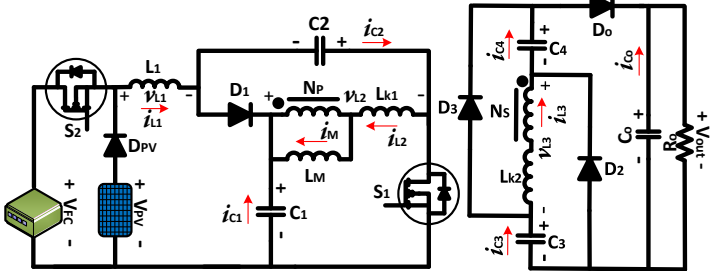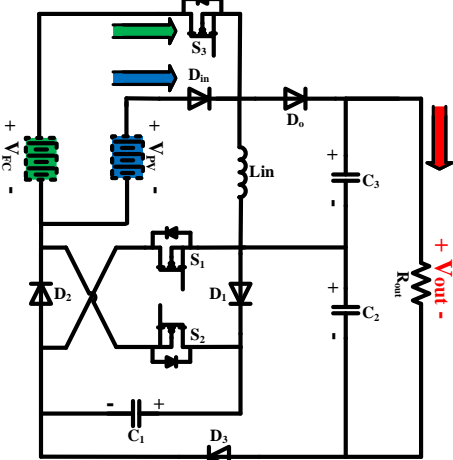
9. Conclusions

This paper has presented a novel DISO high step-up dc-dc converter with modified diodes and switches network, which leads to the creation of an integrated system with high efficiency and high voltage gain for FCEVs applications. The presented structure results in the balanced low voltage stress of output capacitors, diodes and switches. The proposed converter is useful in FCEVs hydride PV/FC battery charger because of its simple structure, high voltage gain, low input current ripple, common ground, and high efficiency. Theoretical calculations for the proposed converter were presented in full detail. The voltage stress of all components and efficiency analysis were provided and the voltage gain was accurately calculated. Finally, the simulation results were carried out in MATLAB/Simulink and agree well with the theoretical analysis of the proposed converter.

As a summary, from the detailed theoretical calculations and simulation results, the following numerical results were extracted from a quantitative point of view:

- The peak efficiency reached 97.4% at half power, and the efficiency at rated power was reported 96%.
- The voltage of the FC is assumed equal to 48V and the voltage of the solar cell is assumed equal to 24V, and also the value of the duty cycle for the first and second MOSFETs is equal to 35% and the value of the duty cycle for the third MOSFET is equal to 15%, then based on simulation results the output voltage value of 218.5V is obtained; which is equal to the theoretical calculations with high accuracy.
- According to the results of theoretical calculations and simulation results, it can be seen that the voltage stresses across capacitors in the proposed converter are very low. The peak voltages of the capacitors indicated by V_{C1}^{Peak}, V_{C2}^{Peak} and V_{C3}^{Peak} are 87.5V, 87.5V and 132.8V, respectively.

A novel transformer-less battery charger based on a new dual-input high step-up DC-DC converter

- The peak voltages of the diodes indicated by V_{Din}^{Peak}, V_{D1}^{Peak}, V_{D2}^{Peak}, V_{D3}^{Peak} and V_{Do}^{Peak} are 23.3V, 85V, 87.2V, 87V and 174V, respectively.

- The peak voltage and average current of the input inductor diodes indicated by V_{Lin} and I_{Lin} are 133.35V and 30A, respectively.

- The output voltage and load current are set to 220V and 4.55A, respectively.

Table 4: Comparison between the proposed DISO high step-up DC-DC converter and related converters

Ref.	Structures	Number of ports	Efficiency (%)	Pros (+ → ■) and Cons (− → ❖)
[2]		One Input/One output	96.9	❖High hardware costs ❖large volume due to the presence of coupled-inductor ■ Continuous input current ■ Double input possibility ■ Low voltage/current stresses on the components
[3]		Two Input/Two output	96.3	❖ High number of components ❖High hardware costs ❖Large volume due to the presence of coupled-inductor ■ Double output possibility ■ Continuous input current
[14]		Two Input/One output	96.3	❖ High number of components ❖High hardware costs ❖Large volume due to the presence of coupled-inductor ■ High voltage gain ■ Magnetically isolated ■ Continuous input current ■ Double input possibility
Proposed Converter		Two Input/One output	97.4	■ High voltage gain ■ Continuous input current ■ Double input possibility ■ Low voltage/current stresses on the components ■ Small volume ■ Low operating cost ■ Simple structure ■ Strong boosting capability ■ Small weight ■ High efficiency

Declaration of Conflicting Interests

The author(s) declared no potential conflicts of interest with respect to the research, authorship, and/or publication of this article.

References

[1] H. Bi, Z. Mu, Y. Chen, Common Grounded Wide Voltage-Gain Range DC–DC Converter With Zero Input Current Ripple and Reduced Voltage Stresses for Fuel Cell Vehicles, IEEE Transactions on Industrial Electronics, Vol.70, No.3, (2022), pp.2607-2616.

[2] P. Bayat, A. Baghramian, A novel self-tuning type-2 fuzzy maximum power point tracking technique for efficiency enhancement of fuel cell based battery chargers, International Journal of Hydrogen Energy, Vol.45, No.43, (2020), pp.23275-23293.

[3] P. Bayat, A. Baghramian, Partly isolated three-port DC–DC converter based on impedance network, IET Power Electronics, Vol.13, No.11, (2020), pp.2175-2193.

[4] H. Matsuo, et al., Characteristics of the multiple-input DC-DC converter, IEEE Transactions on Industrial Electronics, Vol.51, No.3, (2004), pp.625-631.

[5] S. Khosrogorji, et al., Multi-input DC/DC converters in connection with distributed generation units–A review, Renewable and Sustainable Energy Reviews, Vol.66, (2016), pp.360-379.

[6] Y.C. Chen, and Y.C. Liu, Development of multi-port converters for hybrid wind-photovoltaic power system, Proceedings of IEEE Region 10 International Conference on Electrical and Electronic Technology, TENCON 2001 (Cat. No.01CH37239), Vol. 2, (2001).

[7] Y.M. Chen, Y.C Liu, and F.Y Wu, Multi-input DC/DC converter based on the multiwinding transformer for renewable energy applications, IEEE transactions on industry applications, Vol.38, No.4, (2002), pp.1096-1104.

[8] F. Akar, Y. Tavlasoglu and B. Vural, Analysis and experimental verification of a multi-input converter for DC microgrid applications, IET Power Electronics, Vol.11, No.6, (2018), pp.1009-1017.

[9] G. K. Maurya & L. Solankee, Soft-Switched Non-Isolated High Step-Up Three-Port DC-DC Converter for Hybrid Energy Systems with Minimum Switches, IEEE Transactions on Power Electronics, Vol.33, No.12, (2018), pp.10101-10111.

[10] S. Luca, F. Caricchi, F. Crescimbini, O. Honorati, and F. Mezzetti, Performance of a 10kW power electronic interface for combined wind/PV isolated generating systems, In PESC Record. 27th Annual IEEE Power Electronics Specialists Conference, Vol.2, pp. 1027-1032. (1996).

[11] M.R. Feyzi, et al., Brushless DC motor drive based on multi-input DC boost converter supplemented by hybrid PV/FC/battery power system, 24th IEEE Canadian Conference on Electrical and Computer Engineering (CCECE), (2011).

[12] R.J. Wai, et al., Newly designed ZVS multi-input converter, IEEE Transactions on Industrial Electronics, Vol.58, No.2, (2010), pp.555-566.

[13] A. Nahavandi, et al., A nonisolated multiinput multioutput DC–DC boost converter for electric vehicle applications, IEEE Transactions on Power Electronics, Vol.30, No.4, (2014), pp.1818-1835.

[14] P. Bayat, A. Baghramian, Analysis and Control of a New Dual-input Impedance-based DC–DC Converter for Hybrid PV-FC Systems, Advances in Electrical and Computer Engineering, Vol.19, No.4, (2019), pp.47-56.